

Volume 16 • Number 3 • September 2025 • pp. 1–21

DOI: 10.24425/mper.2025.156148



Selected Problems of Effectiveness and Quality in the Dry Rough Milling of Magnesium Alloy AZ91D Using End Mills with Different Helix Angles

Ireneusz ZAGÓRSKI 1 , Jarosław KORPYSA 1 , Monika KULISZ 2 , Agnieszka SKOCZYLAS 1

Received: 05 December 2024 Accepted: 27 July 2025

Abstract

From the point of view of production and manufacturing processes, issues related to surface quality and machining efficiency are very important. This paper presents the results of a study investigating selected problems of quality and efficiency in dry rough milling. Roughness parameters 2D and 3D were analysed. Additionally, 3D surface topography maps and Abbott–Firestone curves were generated. Carbide end mills with different helix angles were used in the study. Experiments were conducted on AZ91D magnesium alloy specimens. The machining process was conducted using high-speed machining parameters. The results showed that the surface roughness of the AZ91D alloy depended to a great extent on the tool geometry and applied machining parameters. Moreover, ANOVA statistical analysis and post-hoc tests (Tukey) were performed to assess the differences between individual groups of the specimens. Additionally, an artificial neural network (ANN) model was developed to predict the Ra parameter, and the results demonstrated its high predictive accuracy (R = 0.966).

Keywords

Manufacturing of magnesium alloy parts, Machining effectiveness, Surface quality, Dry rough milling, Artificial neural networks, ANOVA.

Introduction

Magnesium alloys are now widely used in many industries such as automotive, aerospace and aviation. This is primarily due to their low density, which makes them even lighter than aluminium alloys. The main machining method for light metal alloys is milling (Biruk-Urban et al., 2022). This results from a wide spectrum of possibilities and freedom in shaping the geometry and dimensions of components made from such alloys. The current development in machining techniques makes it possible to conduct subtractive machining processes with both high speed and efficiency (Kuczmaszewski et al., 2016). The main and most visible effect of a machining process is the machined surface condition. Not only does this condition affect the visual aspect of a given component, but it also exerts impact on the operating properties of this component,

Corresponding author: Ireneusz Zagórski – Lublin University of Technology, Faculty of Mechanical Engineering, Department of Production Engineering, Nadbystrzycka 36, 20-618 Lublin, Poland, phone: +48 438 42 40, e-mail: i.zagorski@pollub.pl

© 2025 The Author(s). This is an open access article under the CC BY license (http://creativecommons.org/licenses/by/4.0/)

e.g. friction coefficient, wear rate (El-Shenawy & Farahat, 2023; Krzyzak et al., 2020; Niemczewska-Wójcik & Madej, 2023). It is therefore necessary to ensure that the obtained surface has the most favourable structure, which is usually evaluated based on surface roughness. In many cases, it is possible to predict post-machining surface roughness, but this requires conducting experiments (Savkovic et al., 2020).

The primary way of affecting surface roughness is by changing machining conditions. Varatharajulu et al. (2023) conducted a study on the AZ31 alloy in this regard. The machining process was conducted with variable parameters, demonstrating that the optimum surface roughness was obtained with low cutting parameters. This effect was linked to the low temperature of the cutting tool. Another study related to AZ31 alloy machining (Adhikari et al., 2023) investigated making holes by milling. However, the results showed a completely opposite trend, as the surface roughness decreased with increasing the cutting parameters. For this case, however, surface roughness measurements were made on the lateral surfaces, which might have been the reason for the differences. The authors of the study also attributed the changes in surface texture to a decreased cutting force. The significance of cutting parameters was also described in a study Kumar et

¹ Lublin University of Technology, Department of Production Engineering, Poland

² Lublin University of Technology, Department of Enterprise Organization, Poland

al. (2023) devoted to magnesium alloy ZE41A. Here, increasing the spindle speed also caused a significant reduction in surface roughness, while increasing the feed rate and depth of cut caused an increase in roughness due to higher built-up on the cutting edges. Wang et al. (2023) conducted tests on the ZK61M magnesium alloy. For this material, the use of a higher feed speed also caused surface deterioration due to the formation of troughs and ridges on the surface. Increasing the spindle speed, on the other hand, resulted in smaller and more regular surface irregularities. Similar correlations were also observed in the micro milling of magnesium alloy Mg13Sn (Ercetin et al., 2023). The Sa parameter decreased with decreasing the feed and increasing the cutting speed. This trend was also reflected in changes in the cutting force. The shaping of surface roughness by changing machining conditions is widely used not only in milling, but also in other machining methods such as turning, shot peening or brushing (Kramar & Cica, 2021; Matuszak, 2023; Tomov et al., 2022; Matuszak et al., 2019).

The cutting tool is also a key aspect of the machining process. Tool geometry is of vital importance here, as it significantly affects surface quality (Vukelic et al., 2022), process stability (Bari et al., 2023), chip formation (Ahmed et al., 2023), and post-machining deformation (Zawada-Michałowska et al., 2020, 2022). Hu et al. (2022) investigated the effect of helix angle on the surface roughness of machined titanium alloy TC4. In the study, end mills with different helix angles were used. It was shown that lower surface roughness was obtained by using the end mill with a larger helix angle of $35^{\circ}/38^{\circ}$, while the surfaces milled using the tool with the smallest helix angle of $30^{\circ}/32^{\circ}$ had the worst quality. In addition, the tools had a variable helix – each flute was tilted at a different angle. A similar relationship was established in a work (Sur et al., 2022) which investigated the milling process for titanium alloy Ti6Al4V. For this case, too, the lowest roughness was obtained when using the tool with a variable helix angle of $35^{\circ}/38^{\circ}$. The use of tools with fixed helix angles of 35° and 38°, on the other hand, resulted in the deterioration of surface condition. A more comprehensive analysis was conducted by Xue et al. (2023), who investigated helix, rake and relief angles. The study showed that the most favourable surface structure was obtained when using tools with intermediate values of the angles. In terms of chip formation, it is recommended that the milling process of the AZ91D alloy be conducted using the tool with a smaller helix angle (Zagórski, 2023). The use of tools with the helix angles of 20° and 50° led to the formation of dust, which is the most undesirable chip fraction. However, a greater propensity for the

formation of such chips was observed for the tool with an angle of 50°. In addition to geometry, the material from which the tool is made is also of vital significance. A study Zawada-Michałowska et al. (2023) compared the CFRP composite surface after a milling process that was conducted with polycrystalline diamond and PCD-coated carbide end mills. The use of the coated tool resulted in the roughness parameters being even half lower. The use of protective coatings, however, does not always bring the desired effect, as shown in a study Marakini et al. (2022) on the machining of magnesium alloy AZ91D. The use of both uncoated and TiN-coated carbide tools produced almost similar surface roughness.

Regarding other factors affecting surface quality, one must also mention the way in which the cutting zone is cooled. This is related to the heat generated by the cutting tool. It also affects the cutting forces or strength of the material (Khawaja et al., 2020; Lisowicz et al., 2022). A study Zhang et al. (2023) conducted on the AZ31B magnesium alloy specimens showed that, in contrast to dry machining, the use of fluid could reduce roughness. In some cases, an even better effect could be obtained by using minimum quantity lubrication (MQL). A study Karmiris-Obratański et al. (2022) confirmed that the use of MQL when milling the Incoloy 800 alloy yielded better results than the use of dry milling or flood cooling. The benefits of using the MQL method were also confirmed for the AZ31 alloy (Kanan et al., 2023). The use of a mixture of MQL and biodegradable oils reduced surface roughness and at the same time decreased carbon emissions. More recent developments in this area include cryogenic cooling. Hoverver, Jouini et al. (2023) showed in their study that the use of dry machining and cryogenic cooling produced comparable surface roughness in the machining of the AZ91D alloy.

In recent years, the application of Artificial Neural Networks (ANNs) in modelling surface roughness parameters post-machining has garnered considerable interest (Sangwan et al., 2015; Zagórski et al., 2022). ANNs are highly effective in approximating complex, nonlinear relationships, which offers a critical advantage in materials processing where numerous variables impact the final outcome. This modelling capability is particularly beneficial in the context of machining, where precise surface quality predictions can enhance process optimization, thus reducing the need for extensive, time-consuming experimental trials (Dijmărescu et al., 2021; Kaviarasan et al., 2019).

Previous studies on milling conducted with tools of different geometries have included: dry rough milling of AZ91D/HP by the end mill with different rake angles combined with an analysis of 2D roughness



parameters (lateral and end face) (Gziut et al., 2015) and 3D roughness parameters, A-F curves and 3D maps (end face) (Zagórski, 2024a), dry rough milling of AZ31B by the end mill with different rake and helix angles (end face) together with an analysis of 3D roughness parameters (Zagórski, 2024b). The analyses showed gaps in previous studies, e.g. those related to the milling of the AZ91D alloy using the end mill with variable helix angles.

The existing studies show that ANN models for predicting post-milling surface roughness typically incorporate such input parameters as the cutting speed (v_c) , feed per tooth (f_z) , and the depth of cut (a_p) (Chen et al., 2017; Kulisz et al., 2022b). However, adding the tool helix angle (λ_s) as a variable could enhance prediction accuracy by accounting for the effect on chip shape, cutting forces and process stability. Notably, the helix angles of 20° and 50° generate different forces and heat conditions, thus impacting surface structure. To date, models have been developed for specific tool angles (Zagórski et al., 2022, 2024), yet none of them integrated λ directly in the input variables.

The main objective of this study is to evaluate surface quality depending on the applied end mill helix angle and cutting parameters by the ANOVA analysis of variance and post-hoc tests (Tukey), in order to assess the differences between individual groups of specimens. An important novelty of this study is that it undertakes a comprehensive analysis based on a wide range of roughness parameters (both 2D and 3D), surface topography maps and Abbott-Firestone curves. Also, the assessment is made on both lateral and end faces of the samples. Previous scientific publications lack the analysis of the effect of using variable rake or helix angles on machinability indicators such as surface roughness parameters. The commonly available so-called catalog tools are most frequently used to that end. The proposed geometry is the result of work conducted by the authors at their research center. An additional objective of this study was to develop an ANN model to predict the surface roughness parameter Ra on the end face, based on key input parameters of the cutting process $(v_c, f_z, a_p \text{ and } \lambda_s)$. The ANN model enables accurate prediction of the Ra value, which helps to better understand the influence of individual cutting parameters on surface quality and to optimise the machining process in order to achieve the expected results. The ANOVA variance analysis made it possible to demonstrate whether cutting speed and feed per tooth would significantly affect the Rz roughness parameter. The post-hoc test (Tukey-test) was employed to show whether there would statistically significant differences in the value of the Rz parameter after changing the variables v_c and f_z .

Materials & Methods

The study investigated the rough milling process of magnesium alloy AZ91D that was conducted according to the scheme shown in Fig. 1. Dry machining tests were performed on the Avia VMC800HS milling centre. The study was conducted using cutting tools with a variable helix angle λ_s of 20° and 50°. They were three-flute end mills with a diameter of 16 mm, made of sintered carbide. These tools are not commercially available but were custom made. For maximum stability, the cutter was mounted in the HSK-A63 tool holder (16 × 120 mm holder) and balanced to ISO G2.5 grade with the CIMAT RT 610 balancing machine in accordance with the ISO 21940–11: 2016 standard.

Surface texture examination involved analysing 2D and 3D surface roughness parameters. Also, surface topography maps and Abbott-Firestone curves were generated. All measurements were made with the Hommel Etamic T8000 contact profilometer. The scanning area of sample surface was 4.8×4.8 mm, with a 100 scanning step. The 2D parameters were measured five times per each surface, i.e. the end and lateral faces of the samples. The 2D roughness measurements were conducted with the Hommel Tester T1000 contact profilometer. The measurements were made on the end and lateral faces of the specimens. In addition to the impact of the cutting tool, the relationship between technological parameters and surface roughness was also investigated. The following were made variable: the cutting speed v_c (400–1200 m/min), the feed per tooth f_z (0.05–0.30 mm/tooth) and the axial depth of cut a_p (0.5–6 mm). The radial depth of cut a_e was maintained constant at 14 mm.

The surface roughness parameters, specifically the arithmetical mean roughness parameter (Ra), were modeled using the results of previous experimental investigations. The simulations described in this work were conducted using the Matlab 2023b environment and its Neural Network Application. The artificial neural networks (ANN) were designed with a focus on minimalistic architecture, yielding a single hidden layer in all networks. The number of neurons in this layer ranged from 2 to 15. The architecture comprised one input layer with four neurons that represented the cutting speed v_c , feed per tooth f_z , the axial depth of cut a_p , and helix angle λ_s , as well as one output layer with a single neuron that indicated the surface roughness parameter (Ra) on the end surface of the sample).

Three distinct algorithms were assessed for the training mechanisms: Scaled Conjugate Gradient, Bayesian Regularization and Levenberg—Marquardt. To prevent overfitting during model training, an "early stopping" technique was implemented. This technique stopped the training process after six consecutive increases in the validation error or if there was no reduction in the

error, thereby ensuring that the model would remain effective for future data.

A total of 170 observations of the surface roughness parameters and machining parameters were made during the training procedure. The ratio of data allocation for training, validation and testing was 70:15:15. A single network was chosen for each parameter, and

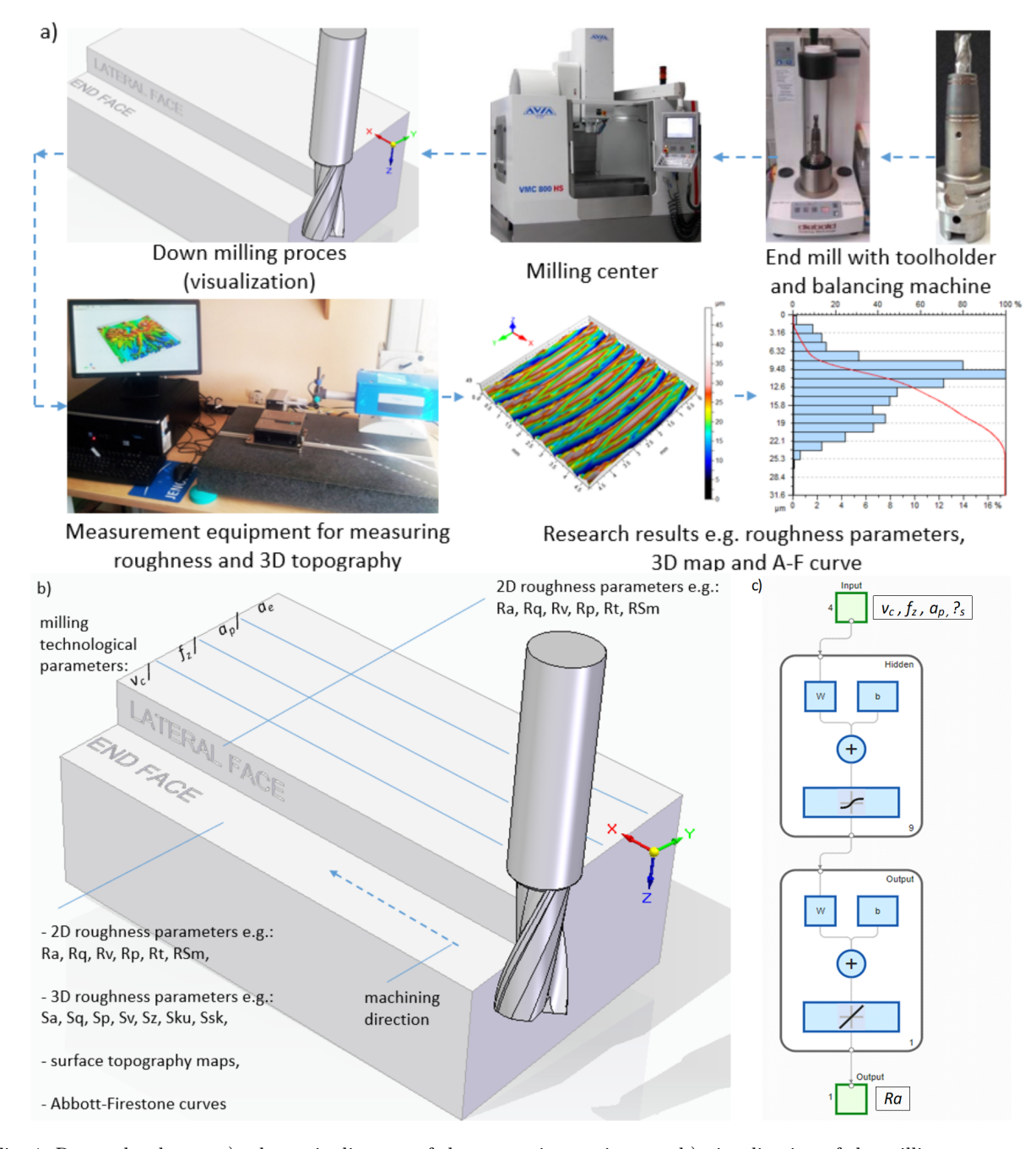


Fig. 1. Research scheme: a) schematic diagram of the measuring equipment, b) visualization of the milling process with a roughness measurement model for the lateral and end face of the workpiece and c) schematics of the artificial neural network



numerous networks were modeled. The qualitative metrics detailed in Table 1 were employed to evaluate the reliability and performance of the networks.

Table 1 Quality metrics

Quality Indicator	Formula
Regression value R	$R(y', y^*) = \frac{\operatorname{cov}(y', y^*)}{\sigma_{y'}, \sigma_{y^*}}, R \in \langle 0, 1 \rangle$
Mean Squared Error (MSE)	$MSE = \frac{1}{n} \sum_{n=1}^{n} (\hat{y}_i - y_i)^2$
Root Mean Square Error (RMSE)	$RMSE = \sqrt{\frac{\sum_{n=1}^{n} (y_i - \hat{y}_i)^2}{n}}$
Mean Absolute Error (MAE)	MAE = $\frac{1}{N} \sum_{i=1}^{N} (y_i - \hat{y}_i)^2$

Meaning of Symbols:

 $\sigma_{y'}$ – standard deviation of the measured Ra parameter,

 $\sigma_{y^*}^{\sigma}$ - standard deviation of the predicted Ra parameter,

 y_i – the measured Ra parameter,

 \hat{y}_i – the value of the Ra parameter for the i-th observation obtained from the model

Results

Helix angle λ_s versus 2D roughness parameters

The effect of cutting speed and helix angle on 2D surface roughness parameters is presented in Figs. 2–4.

Lower values of the parameters Rv, Rp and Rt (Fig. 2) were obtained on the lateral surfaces. These surfaces were also characterised by a more symmetrical distribution of peaks and valleys. On the end face of the sample, the distribution of peaks and valleys changed with the cutting speed. For most cases, lower parameters were obtained on both the end face and lateral surface when the machining process was conducted with a larger helix angle tool. A change in the cutting speed had no clear effect on the obtained values of surface roughness parameters.

Similar relationships were also observed for the parameters Ra and Rq (Fig. 3), where a change in the cutting speed had no clear effect on the values of the analysed parameters. Again, however, the parameters were several times lower when the machining process

was conducted on the lateral surfaces. For both machining cases, lower roughness values were mostly obtained for the tool angle of $\lambda_s = 50^{\circ}$, and the difference was particularly pronounced on the end face of the samples.

A different trend could be observed for the RSm parameter (Fig. 4), which reached lower values on the end face of the samples. The end faces of the samples were also characterised by a smaller scatter of the RSm values. Lower roughness values were again obtained on the end face of the samples for the tool with a larger helix angle, while the results obtained for the lateral surfaces were similar irrespective of the tool used. Again, a change in the cutting speed had no significant effect on the RSm parameter values.

Feed per tooth had a much greater impact on surface roughness. The parameters Rv, Rp and Rt(Fig. 5) increased over the entire range of the tested feed per tooth values. This change was observed for the end and lateral surfaces alike, but on the lateral surfaces of the samples the values of the roughness parameters were considerably lower, especially when higher feeds per tooth were used. On the end face of the samples, lower roughness values were predominantly obtained using the tool with a smaller λ_s angle, which is a different trend compared to that observed for the cutting speed. On the lateral surfaces, however, lower values of the roughness parameters at low feed rates $(f_z = 0.05 - 0.15 \text{ mm/tooth})$ were obtained for the tool with a smaller λ_s angle, while at higher feed rates $(f_z = 0.20 - 0.30 \text{ mm/tooth})$ for the tool with a greater λ_s angle.

Similar relationships were observed for the parameters Ra and Rq (Fig. 6). The values of these parameters again increased over the entire tested range of feed per tooth, while lower values were measured on the lateral surfaces. Similarly to the Rv, Rp and Rt parameters, the effect of the helix angle on Ra and Rq depended on the feed per tooth. At low feed rates, the obtained values of the Ra and Rq parameters were lower when the machining process was conducted using the tool with a greater helix angle. In contrast, at higher feed rates, the Ra and Rq values were lower for the tool with a smaller angle, and the decrease in their values was more pronounced. Regarding the end face of the samples, it is impossible to determine which tool produced more favourable results since the machining result depended on the feed per tooth.

The use of a higher feed per tooth value also resulted in an increase in the RSm parameter (Fig. 7). However, similarly to the impact of the cutting speed, the obtained RSm parameter values were lower on the end faces of the samples. The results for both tools varied with feed per tooth. Regarding the lateral surface, on the other hand, the RSm values were

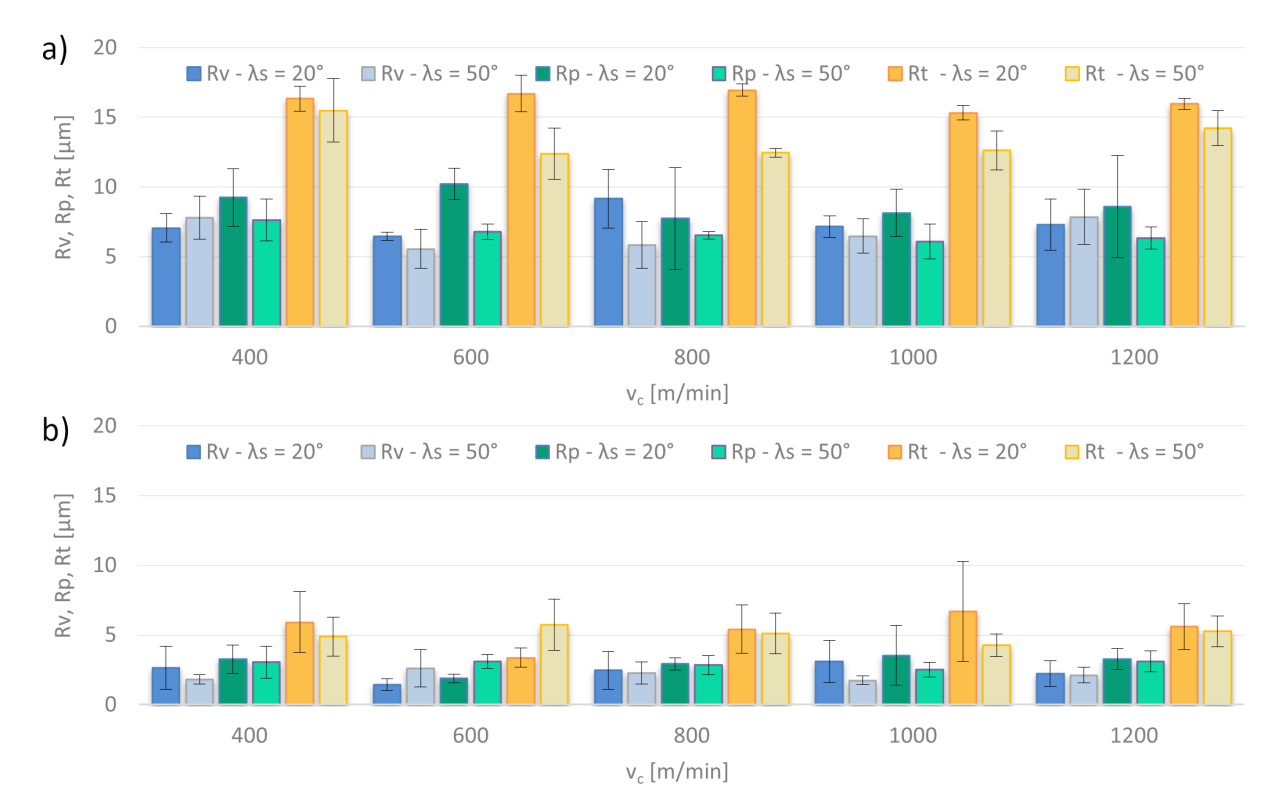


Fig. 2. Cutting speed versus roughness parameters Rv, Rp and Rt on the surface of a sample: a) end face, b) lateral face

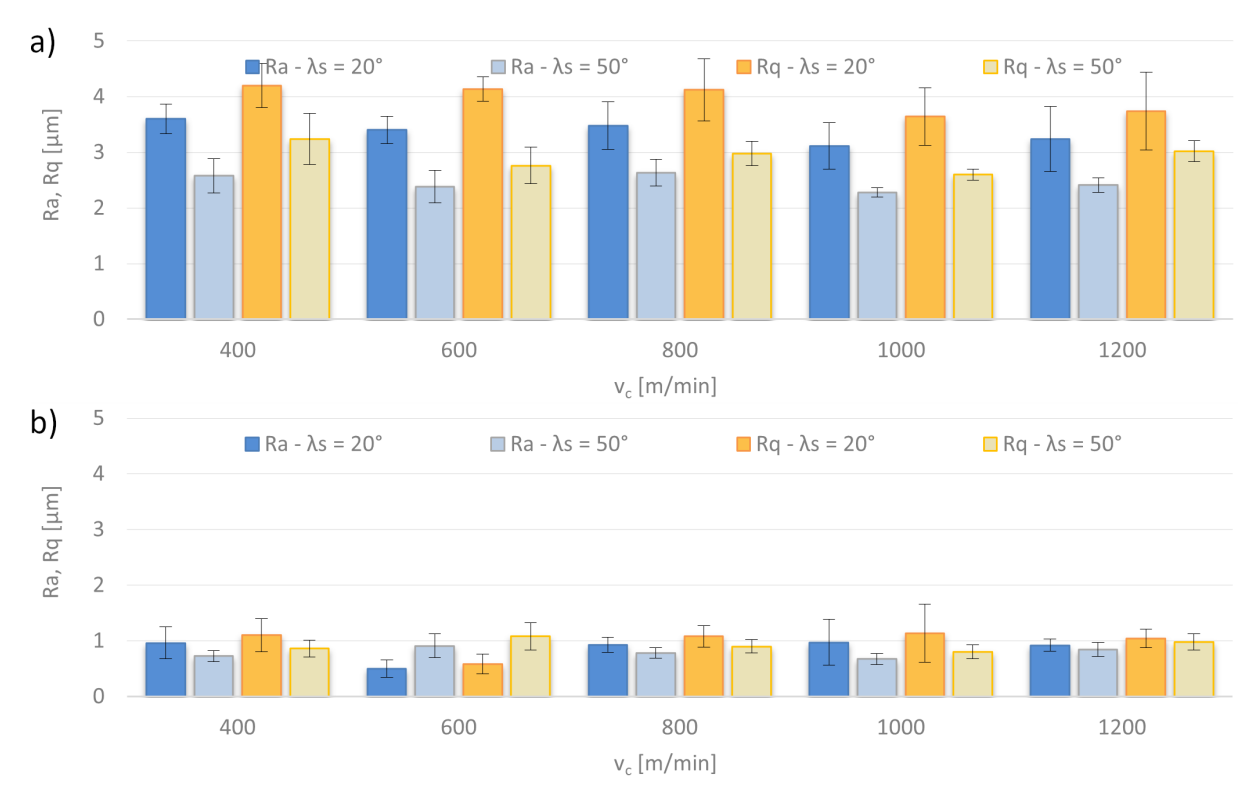


Fig. 3. Cutting speed versus roughness parameters Ra and Rq on the surface of a sample: a) end face, b) lateral face

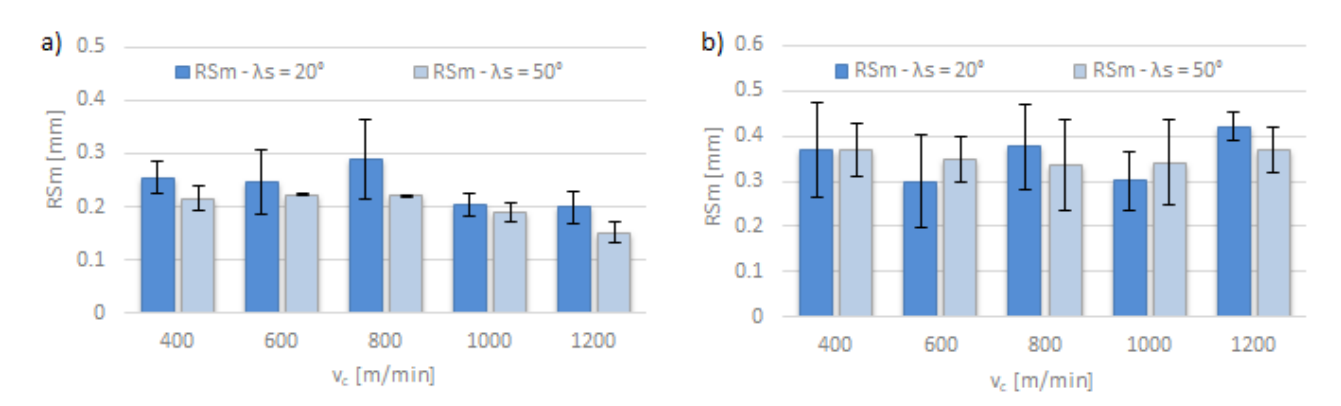


Fig. 4. Cutting speed versus RSm parameter on the surface of a sample: a) end face, b) lateral face

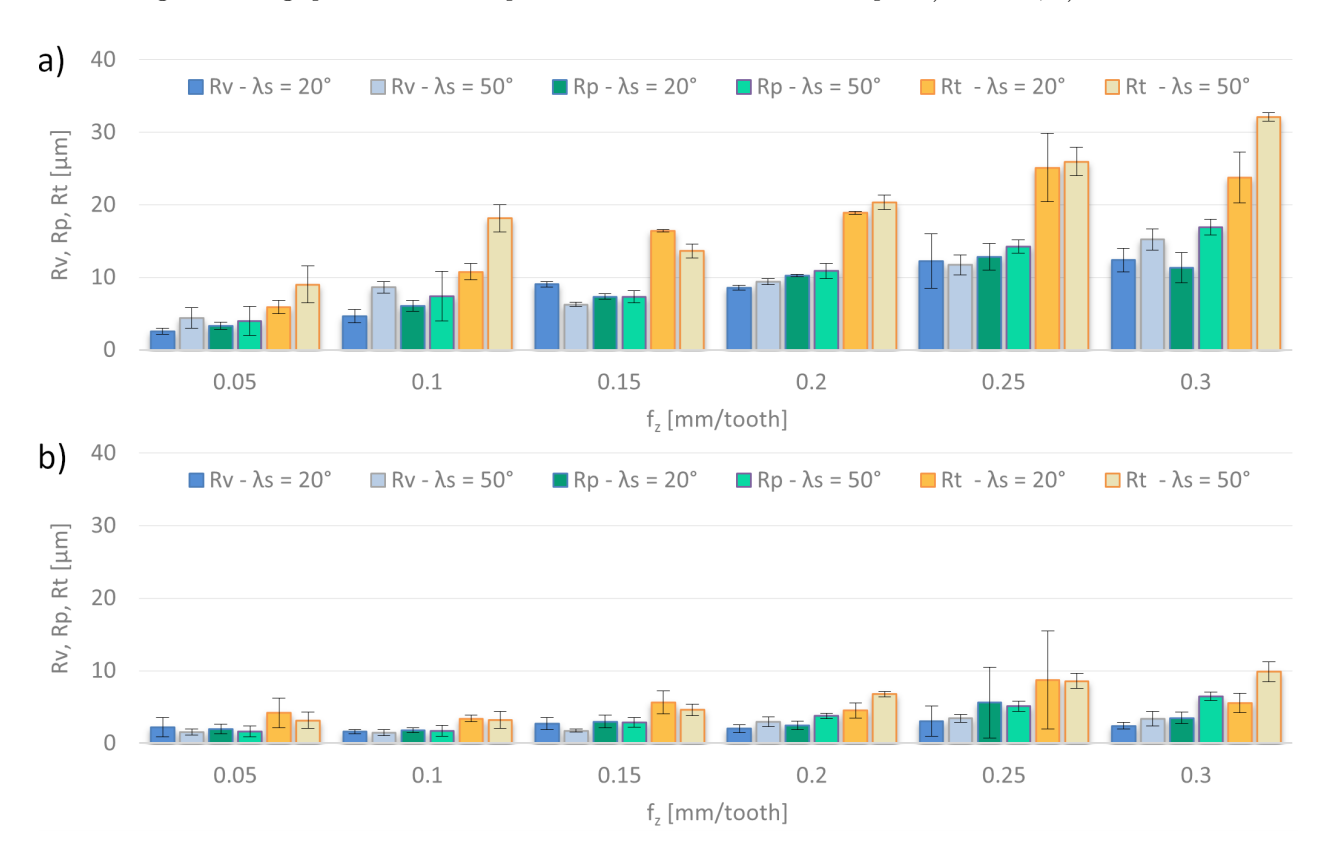


Fig. 5. Feed per tooth versus roughness parameters Rv, Rp and Rt on the surface of a sample: a) end face, b) lateral face

lower for the tool with a smaller helix angle, and the differences in the results were most pronounced when the machining process was conducted with high feeds ($f_z = 0.20 - 0.30 \text{ mm/tooth}$).

When the axial depth of cut was changed, the surface roughness parameters were only measured on the end face of the sample. This was due to the insufficient height of the lateral surfaces, which made the measurements impossible. The values of the parameters Rv, Rp and Rt (Fig. 8) remained at similar levels, regardless of the applied value of the axial depth of cut. For most cases,

these parameters were lower for the tool with a smaller helix angle, but the differences between the tools were relatively small. Despite changing the values of the Rv and Rp parameters, the machined surfaces had a fairly uniform structure, with no dominant high peaks or valleys.

Considering the roughness parameters Ra and Rq (Fig. 9), a more favourable effect was obtained by using the tool with a smaller helix angle. This, however, only applied to smaller depths of cut ranging 1–3 mm, because at larger axial depths of cut, the

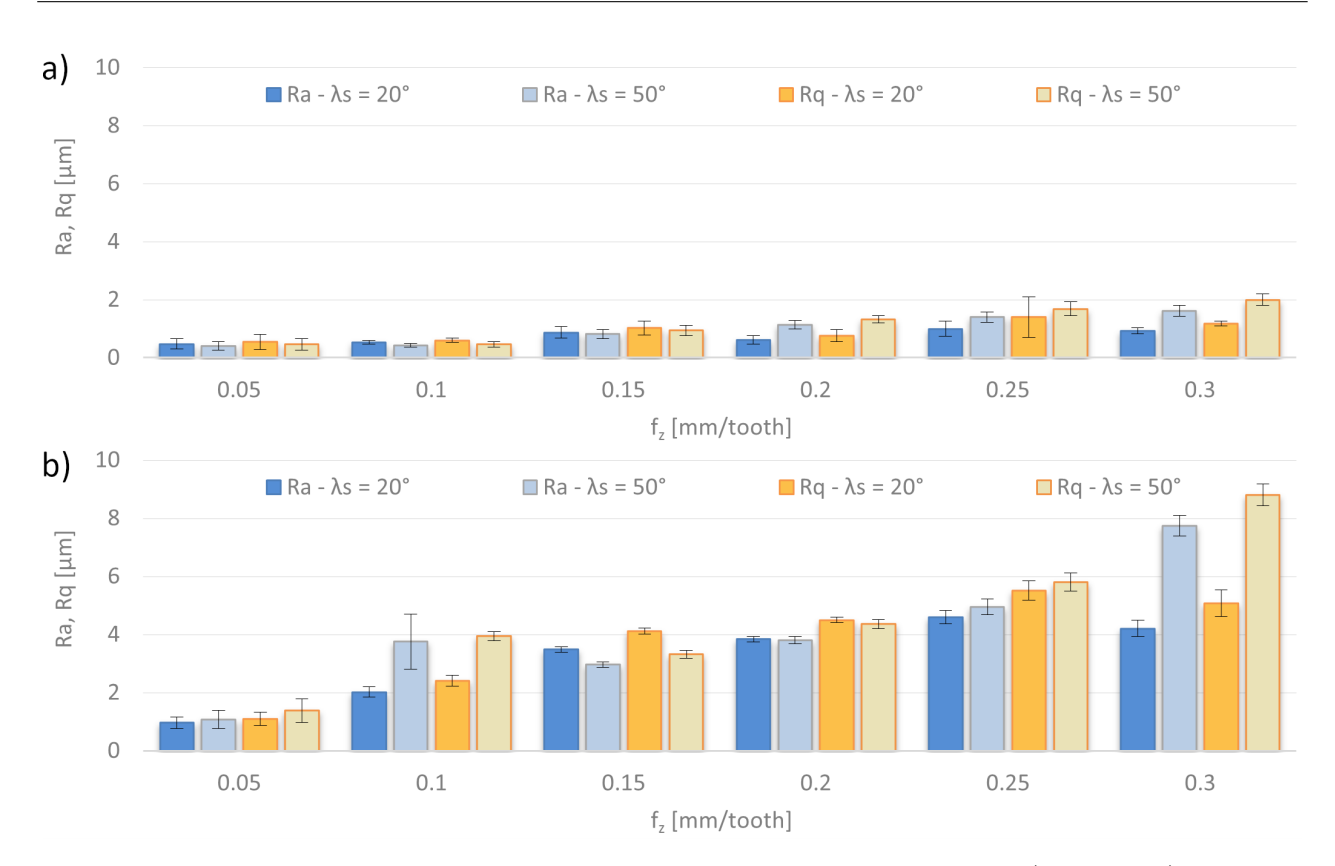


Fig. 6. Feed per tooth versus roughness parameters Ra and Rq on the surface of a sample: a) end face, b) lateral face

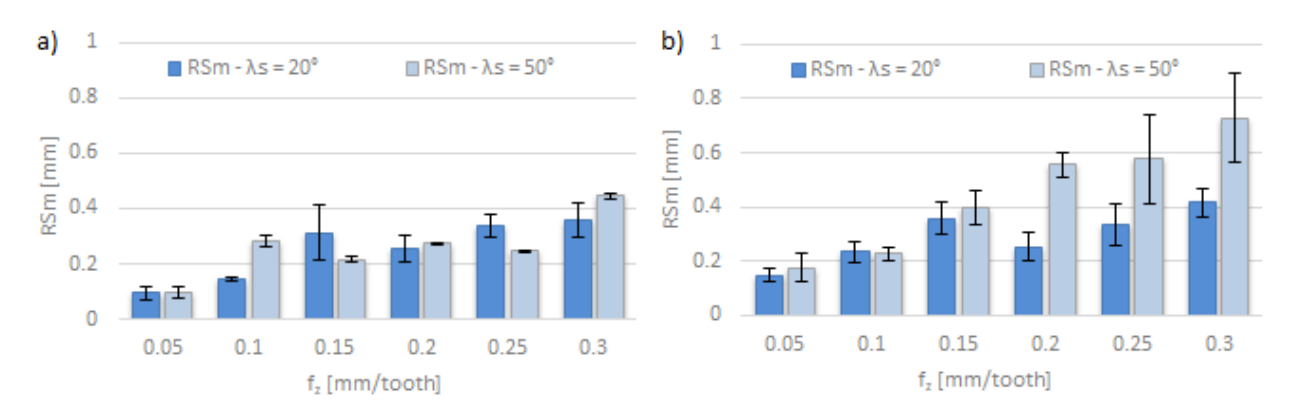


Fig. 7. Feed per tooth versus roughness parameter RSm on the surface of a sample: a) end face, b) lateral face

values of these parameters were comparable, regardless of the tool used. A change in the axial depth of cut value had no evident effect on the Ra and Rq parameters when the machining process was conducted with the helix angle $\lambda_s = 50^{\circ}$, since their values remained similar over the entire tested axial depth of cut range.

A similar effect was observed for the RSm parameter (Fig. 10). Its values were also very similar regardless of the applied depth of cut value, when the machining

process was carried out using the tool with a greater helix angle. The most pronounced change occurred when the machining process was conducted with the highest depth of cut, i.e. $a_p=6~\mathrm{mm}$, which led to a marked increase in the RSm parameter. The same was also observed for the surfaces machined with the other tool. However, for this tool, the values of RSm gradually increased as a result of using the higher depth of cut value.

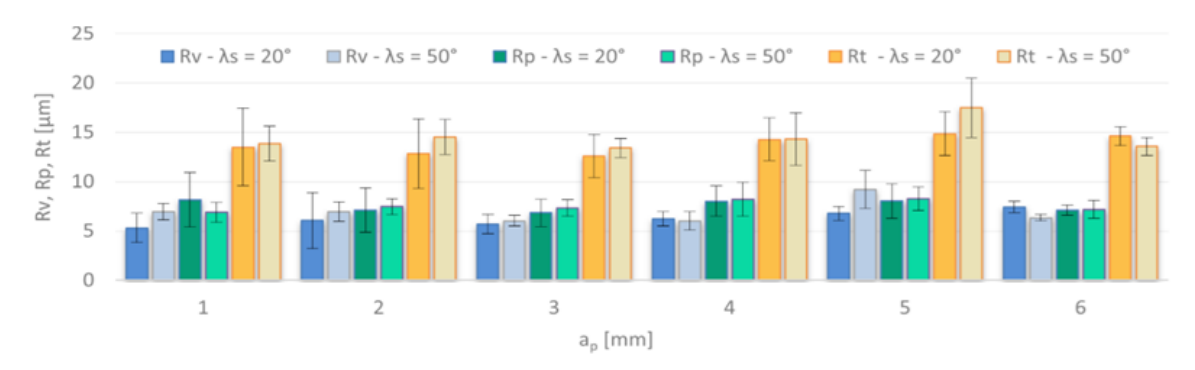


Fig. 8. Axial depth of cut versus roughness parameters Rv, Rp and Rt on the end face of a sample

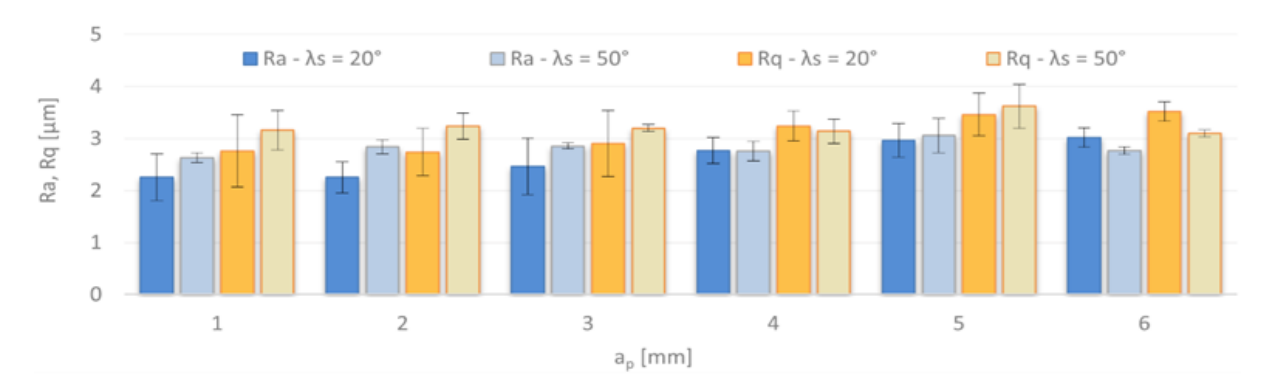


Fig. 9. Axial depth of cut versus roughness parameters Ra and Rq on the end face of a sample

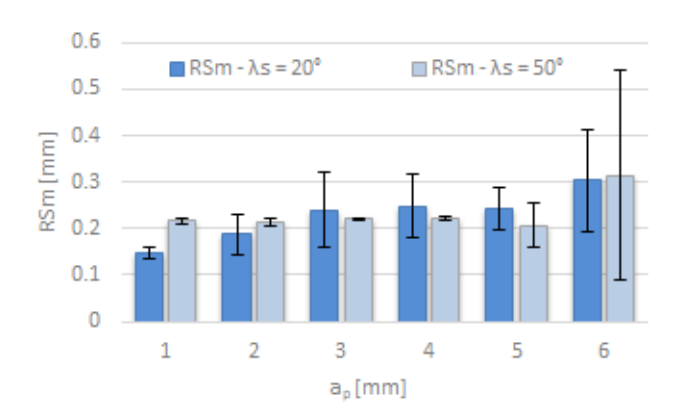


Fig. 10. Axial depth of cut versus roughness parameter RSm on the end face of a sample

ANOVA analysis

A one-way analysis of variance ANOVA (significance level $\alpha=0.05$) was employed to assess the significance of the impact of the technological parameters of milling (cutting speed v_c and feed per tooth f_z) on the Rz roughness parameter. The analyzed variable had a normal distribution, which was confirmed by the Shapiro-Wilk test, and the variances were homogeneous, as verified with the Levene test.

An analysis of the ANOVA results (Table 2) demonstrates that the use of the 20° helix angle produced statistically significant differences in the mean value of the Rz parameter for the variable cutting speed (Fig. 11) and feed per tooth (Fig. 12). As for the 50° helix angle, the ANOVA analysis results showed statistically significant differences in the Rz parameter value with varying the feed per tooth (Fig. 12).

Table 2 ANOVA analysis of variance for the surface roughness parameter Rz over the applied cutting speed and feed per tooth ranges, considering the helix angle

	Rz – helix angle 20°					
	DF	SS	MS	F	p	
$v_{ m c}$	4	9.3023	2.2356	20.588	0.0000	
f_{z}	5	11.1723	2.2345	26.577	0.0000	
	Rz – helix angle 50°					
$v_{ m c}$	4	0.7968	0.1992	2.346	0.1016	
f_{z}	5	112.0123	22.4025	167.226	0.0000	

where: DF – number of the degrees of freedom, SS – sum of squares between groups, MS – mean sum of squares between groups, F – value of the test statistic, p – probability level

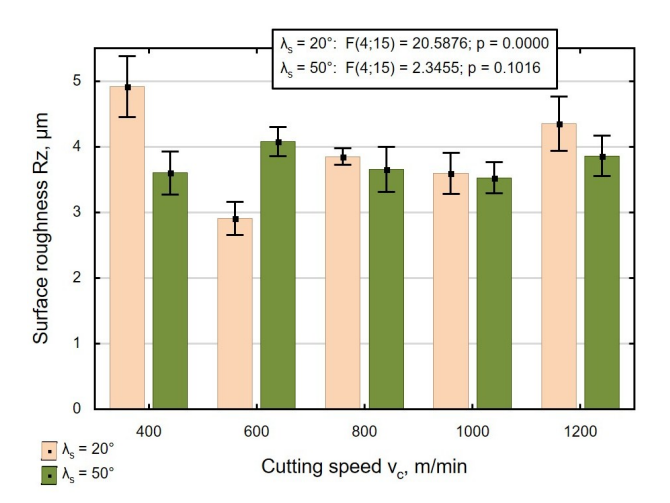


Fig. 11. Effect of the cutting speed on the surface roughness parameter Rz

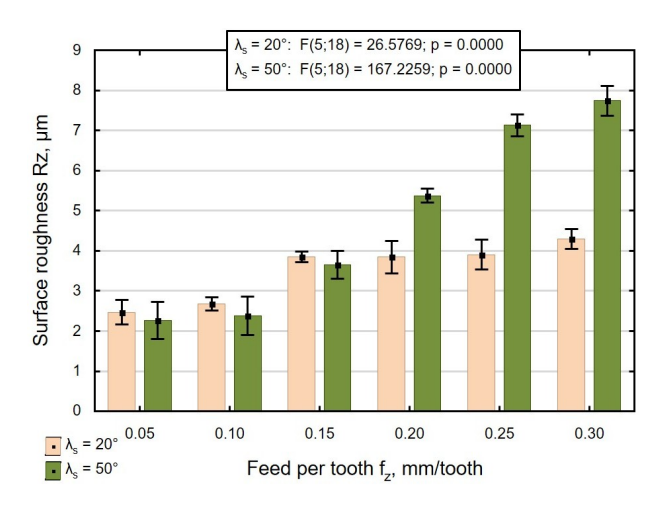


Fig. 12. Effect of the feed per tooth on the surface roughness parameter Rz

In the milling process conducted with both variable feed per tooth and cutting speed using the 20° helix angle and in the milling process conducted with a variable fz using the 50° helix angle, the probability level p was lower than the adopted significance level ($\alpha=0.05$), whereas the values of the test statistics $F_{(5;18)}$ and $F_{(4;15)}$ were higher than the adopted F_{α} .

The results of the ANOVA analysis of variance demonstrated statistically significant differences in the mean values of the roughness parameter Rz between the analysed groups. The post-hoc test (Tukey test) was employed to verify which of the compared groups differed statistically significantly.

In Table 3 are listed the results of the Tukey test for the dependent variable Rz. The red color indicates the level of probability for which there are no statistically significant differences. An analysis of the data shows that changing the cutting speed from 400 m/min to 1200 m/min and from 600 m/min to 1000 m/min, as well as from 800 m/min to 1000 m/min and from 800 m/min to 1000 m/min does not statistically significantly affect the value of the surface roughness parameter Rz for the milling process conducted with the 20° helix angle tool. Regarding the effect of feed per tooth on the dependent variable Rz, statistically significant differences were only observed when the feed per tooth was varied from 0.05 mm/tooth to 0.15; 0.20; 0.25 and 0.30 mm/tooth and from 0.10 mm/tooth to 0.15; 0.20; 0.25 and 0.30 mm/tooth.

The statistical analysis results of the roughness parameter Rz after milling conducted with the 50° helix angle tool revealed that changing the feed per tooth from 0.05 mm/tooth to 0.10 mm/tooth and from 0.25 mm/tooth to 0.30 mm/tooth did not significantly affect the analysed dependent variable (Table 4).

Table 3

Comparative analysis of the significance of differences (post-hoc Tukey test) between the mean values of the Rz roughness parameter after a milling process conducted with a 20° helix angle tool and different technological parameters (variable cutting speed and feed per tooth)

Rz – helix angle 20°

Cutting speed [m/min]

$v_{ m c}$	400	600	800	1000	1200
400		0.0001	0.0033	0.0005	0.1692
600	0.0001		0.0092	0.0703	0.0003
800	0.0033	0.0092		0.8173	0.2685
1000	0.0005	0.0703	0.8173		0.0424
1200	0.1692	0.0003	0.2685	0.0424	

Feed per tooth [mm/tooth]

$f_{\mathbf{z}}$	0.05	0.10	0.15	0.20	0.25	0.30
0.05		0.8993	0.0001	0.0001	0.0001	0.0001
0.10	0.8993		0.0003	0.0003	0.0002	0.0001
0.15	0.0001	0.0003		1.0000	0.9997	0.2980
0.20	0.0001	0.0003	1.0000		0.9994	0.2769
0.25	0.0001	0.0002	0.9997	0.9994		0.4389
0.30	0.0001	0.0001	0.2980	0.2769	0.4389	



Table 4

Comparative analysis of the significance of differences (post-hoc Tukey test) between the mean values of the Rz roughness parameter after a milling process conducted with a 50° helix angle tool and variable feed per tooth

	Rz – helix angle 50°						
	Feed per tooth [mm/tooth]						
$f_{\mathbf{z}}$	0.05	0.10	0.15	0.20	0.25	0.30	
0.05		0.9983	0.0006	0.0001	0.0001	0.0001	
0.10	0.9983		0.0013	0.0001	0.0001	0.0001	
0.15	0.0006	0.0013		0.0001	0.0001	0.0001	
0.20	0.0001	0.0001	0.0001		0.0001	0.0001	
0.25	0.0001	0.0001	0.0001	0.0001		0.2300	
0.30	0.0001	0.0001	0.0001	0.0001	0.2300		

Helix angle λ_s versus 3D roughness parameters

Figure 13 shows the effect of cutting speed and helix angle on 3D surface roughness parameters.

Considering the tools with different helix angles, higher values of the analysed 3D roughness pa-rameters (Sa, Sq) were obtained for the tool with a helix angle of 50°. This situation changes for the Sp, Sv, Sz and Sku parameters with varying the cutting speed. In addition, an increase in the cutting speed does not reveal a clear trend related to an increase or decrease in all surface roughness parameters. These results should be discussed separately. An increase in the cutting speed causes an increase in the values of Sa and Sq, regardless of the tool used. A similar relationship can be observed for the parameters Sp and Sv, but only for the 50° helix angle tool. On the other hand, a different situation can be observed for the parameters Sv and Spwhen the helix angle is set equal to 20° and the cutting speed is variable. For this particular case, an increase in the cutting speed causes a decrease in the values

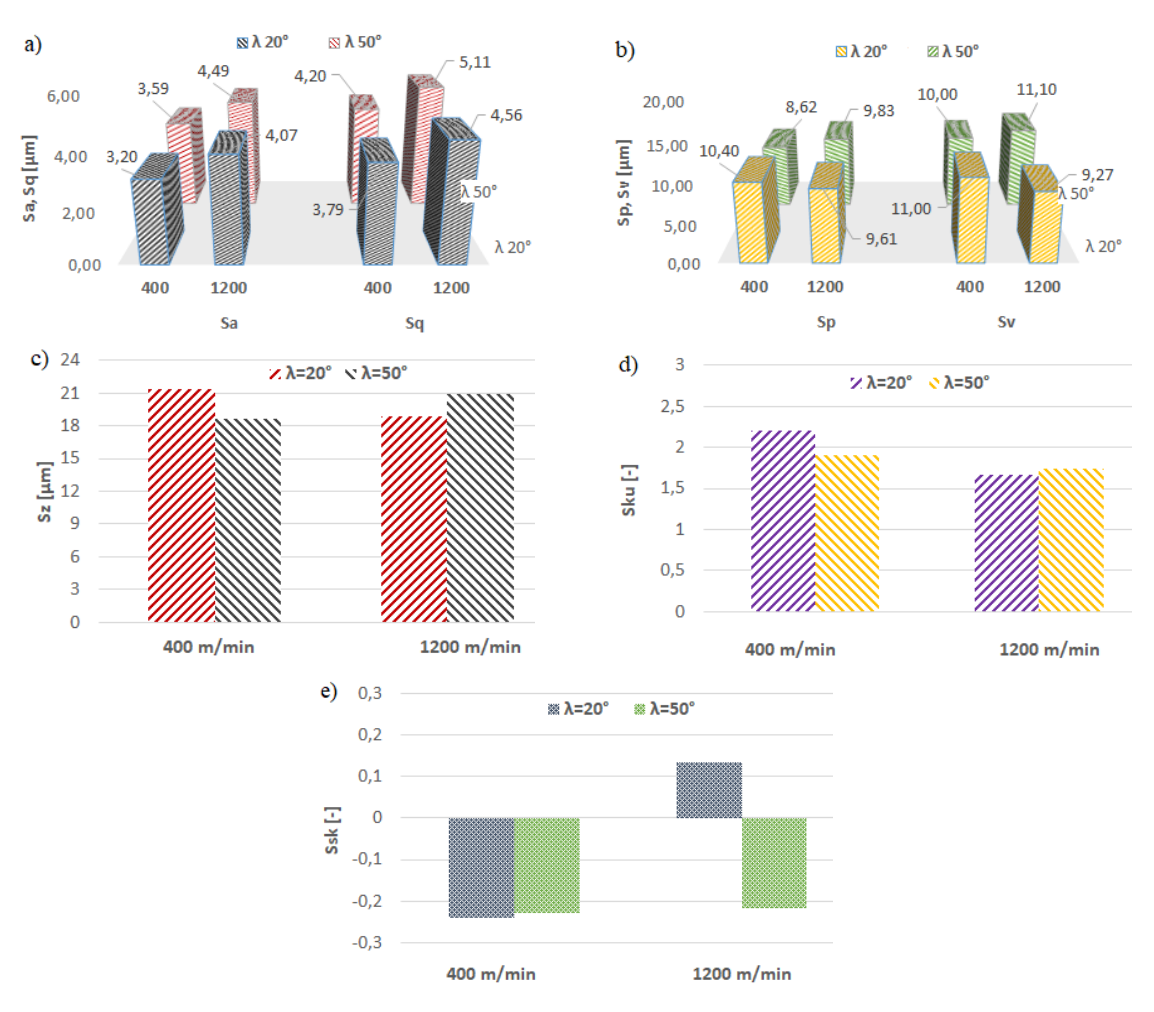


Fig. 13. Cutting speed and helix angle versus roughness parameters: a) Sa, Sq, b) Sp, Sv, c) Sz, d) Sku, e) Ssk

of both analysed 3D surface roughness parameters. It is also difficult to observe a clear trend for the Sz parameter. An analysis of the functional parameters of the surface, namely skewness and kurtosis, reveals that the Sku values are below 3; hence, it can be concluded that the peaks and grooves are rounded. In general, it can be assumed that for both tools, the Sku parameter takes similar values. On the other hand, an analysis of the Ssk parameter reveals two separate trends. For a lower cutting speed, the Ssk parameter takes negative values, which may indicate a higher frequency of deep valleys (defined as a plateau, which is considered optimal). On the other hand, with a higher cutting speed, Ssk assumes negative values for the 50° helix angle and a positive value for the 20° helix angle. In general, the values of the roughness parameters in question range as follows: approx. 3.20-5.11 μ m for Sa and Sq, approx. 8.62–11.10 μ m for Spand Sv, and approx. 18–21 μ m for Sz.

Figure 14 shows the effect of feed per tooth and helix angle on 3D surface roughness parameters. It can easily be observed that an increase in the feed per tooth usually causes an increase in the 3D surface roughness. This relationship can be observed for the parameters Sa, Sq and Sz and the 20° helix angle tool. This can be explained by an increased cross section of the removed layer, which is even more evident when the machining process is conducted using the extreme values of the machining parameters. For most cases, higher roughness parameters were obtained on the surfaces that were machined using the 50° helix angle tool. One exception is the case when the machining process was conducted with the feed per tooth value set equal to 0.05 mm/tooth (Sp, Sv and Sz parameters). Regarding the functional parameters, i.e. skewness and kurtosis, the following can be observed: for most cases, the Sku parameter takes values below 3, which may prove that the peaks and grooves are

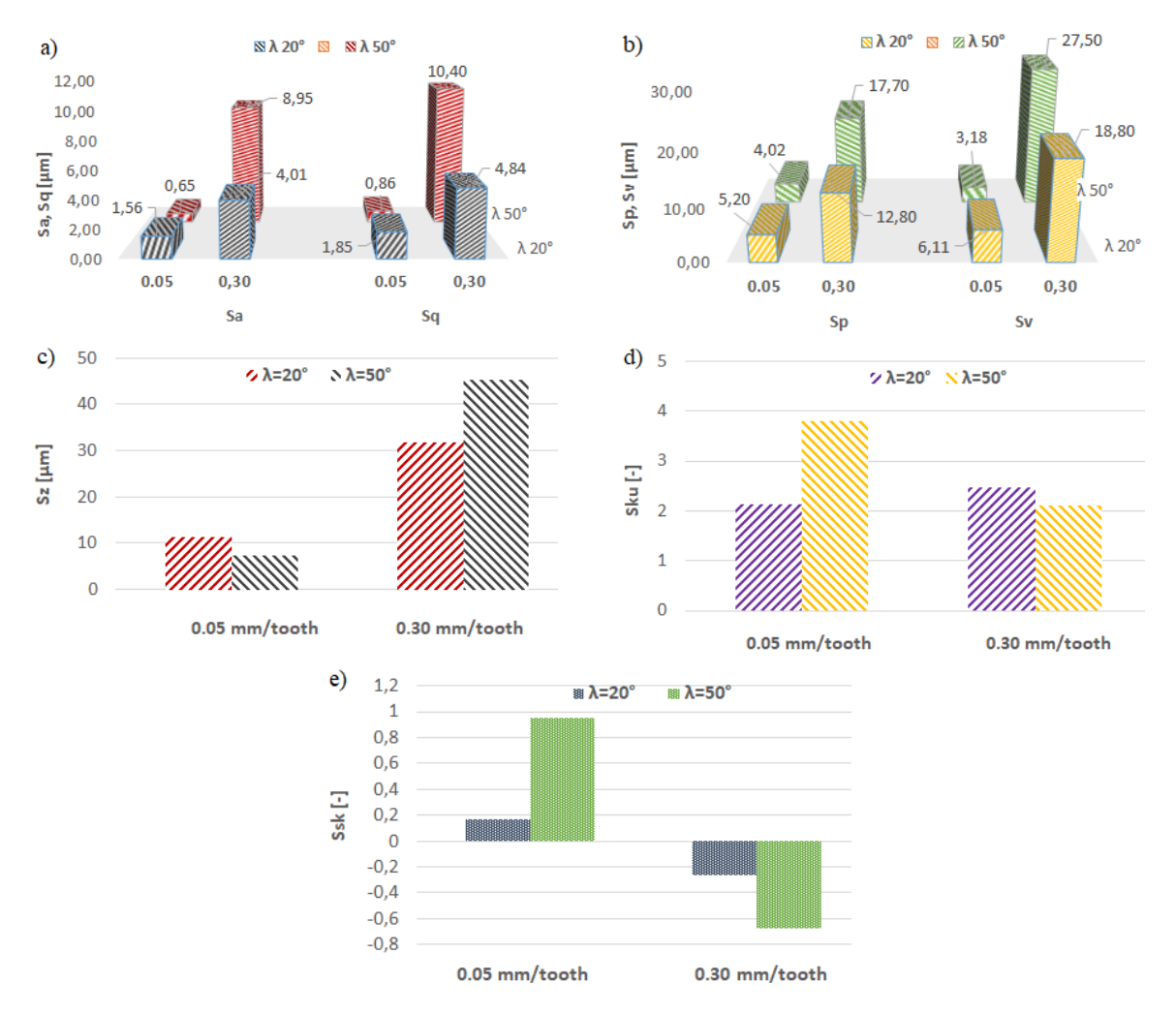


Fig. 14. Feed per tooth and helix angle versus roughness parameters: a) Sa, Sq, b) Sp, Sv, c) Sz, d) Sku, e) Ssk

rounded. The exception to this trend was the case when the feed per tooth was 0.05 mm/tooth and the helix angle was 50° (the skewness was 3.79). The kurtosis takes positive values (for the feed per tooth equal 0.05 mm/tooth) as well as negative values (for the feed per tooth equal 0.30 mm/tooth). The negative values may indicate a higher frequency of deep valleys (defined as a plateau, which is considered optimal). The positive values (surfaces with positive skewness values) show good adhesion resistance. The values of the roughness parameters ranged as follows: from $0.86 \text{ to } 10.4 \text{ }\mu\text{m}$ for Sa and Sq (which is a relatively wide range for these parameters), from $3.18 \text{ to } 27.50 \text{ }\mu\text{m}$ for Sp and Sv, and from approx. $10 \text{ to } 45 \text{ }\mu\text{m}$ for Sz.

Figure 15 shows the effect of cutting speed and helix angle on 3D surface roughness parameters. It can be observed that an increase in both the axial depth of

cut and the helix angle led to higher values of the Saand Sq parameters. The values of these parameters ranged from 2.41 to 5.07 µm. The only exception was the Sq parameter for the machining process conducted with the 50° helix angle tool. A similar situation was also observed for the Sv parameter, where an increase in a_n resulted in a higher value of Sv. The values of this parameter ranged between 7.84 and 11.30 µm. On the other hand, a different situation occurred for the Sp parameter, where its value decreased. The values of this parameter ranged between 6.79 and 13.20 μ m. As for the Sz parameter, its value descreased with increasing the axial depth of cut. The Sz parameter value ranged from approx. 16 to approx. 25 μm. The skewness parameter took values below 3, which may indicate that the peaks and grooves are rounded. Similarly, the kurtosis parameter took positive values when

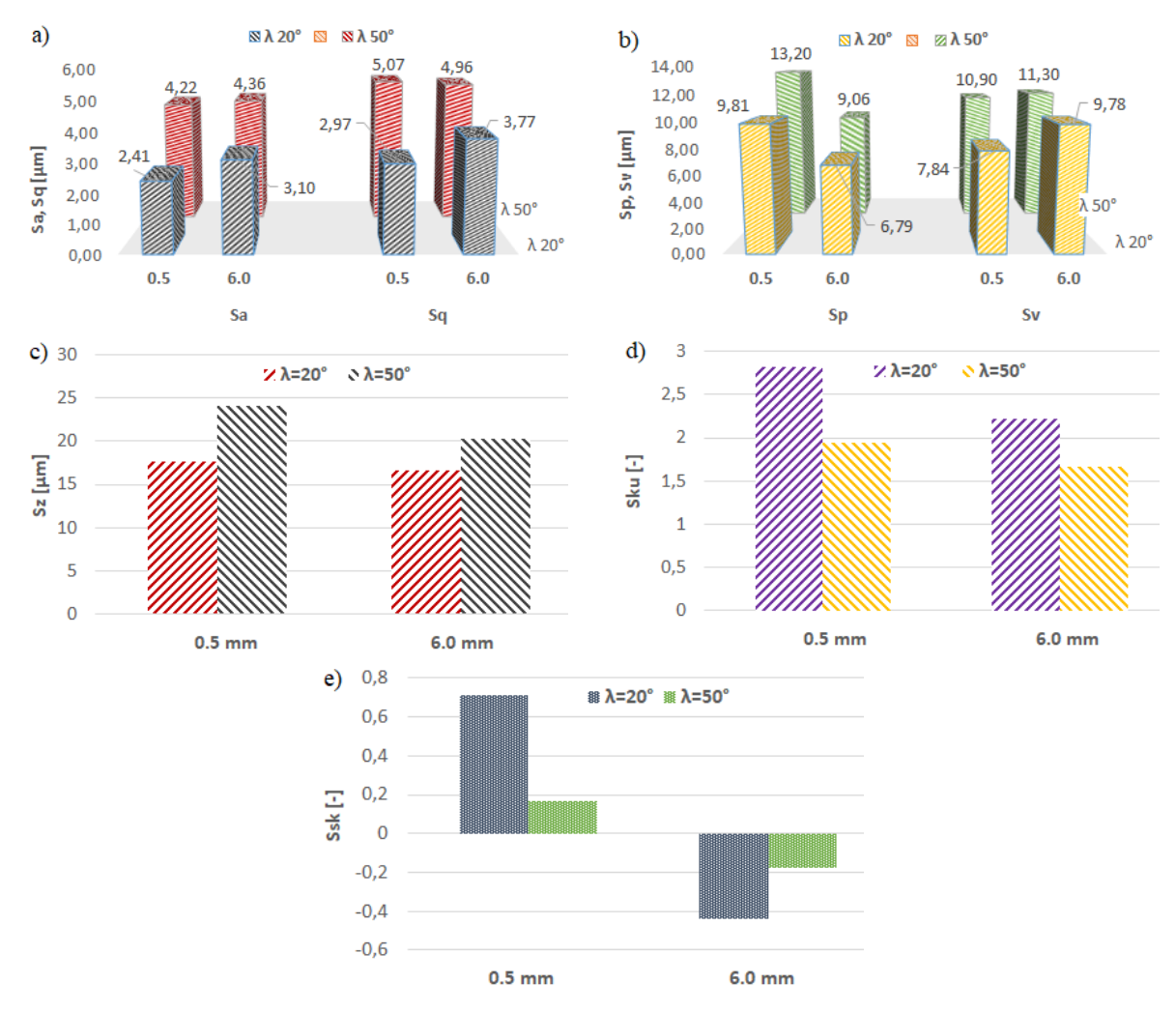


Fig. 15. Axial depth of cut and helix angle versus roughness parameters: a) Sa, Sq, b) Sp, Sv, c) Sz, d) Sku, e) Ssk

the axial depth of cut was 0.5 mm. However, an opposite situation could be observed when using a higher value of the axial depth of cut. Here, the parameter Ssk took negative values, which may indicate a higher frequency of deep valleys (defined as a plateau, which is considered optimal).

Helix angle λ_s versus selected surface topography maps and Abbott–Firestone curves

Table 5 also shows examples of surface topography maps obtained for both tools and extreme values of the technological parameters. Both types of end mills produced surfaces with clearly visible machining marks left by the tool, which is mainly due to the use of high values of the technological parameters. The primary difference to be observed is the overlapping of the machining marks left by the tool with a smaller helix angle. As a result of using this tool, the peaks and valleys on the surface had a more uniform shape, while the surfaces machined using the tool with a helix angle of 50° showed numerous irregularities in the form of grooves.

Table 6 shows examples of Abbott–Firestone curves obtained for the tools with different helix angles (similarly to the surface topography maps, they were plotted for extreme values of the technological machining parameters). These curves may provide important data in terms of surface performance. In general, the curves of a progressive or a progressive-digressive shape are considered favourable. Based on Abbott–Firestone curves, one may draw inferences about the

resistance of a given surface to e.g. tribological wear (a curve of progressive shape means that the analysed surface has rounded peaks of micro irregularities and is thus more resistant to wear).

An analysis of the curves plotted for the tested cutting speeds and axial depths of cut reveals that these curves have approximately a proportional shape. The shape of the curves obtained for the tested feed per tooth is approximately degressive-progressive (for a helix angle of 20°) or progressive (for a helix angle of 50°). As for the tested axial depth of cut, the shape of the curves is progressive (for a helix angle of 20°) and approximately proportional (for a helix angle of 50°).

Modeling the Ra roughness parameter (on the end face of the specimen)

Optimal outcomes were achieved by applying the Levenberg–Marquardt training method, regardless of the variations in complexity and precision. The Ra model, with 9 neurons in its hidden layer, concluded its training after 123 epochs, attaining the optimal validation performance at epoch 123 (0.089). The specific results of this neural network model and the network quality metrics are presented in Table 7.

The quality metrics of the ANN model developed for predicting the surface roughness parameter Ra demonstrates solid performance. With a high correlation coefficient R of 0.966, the model shows a strong fit across the entire dataset. Regression plots for the training, validation and overall datasets are presented below

Table 5
3D images of the surfaces obtained using tools with different helix angles

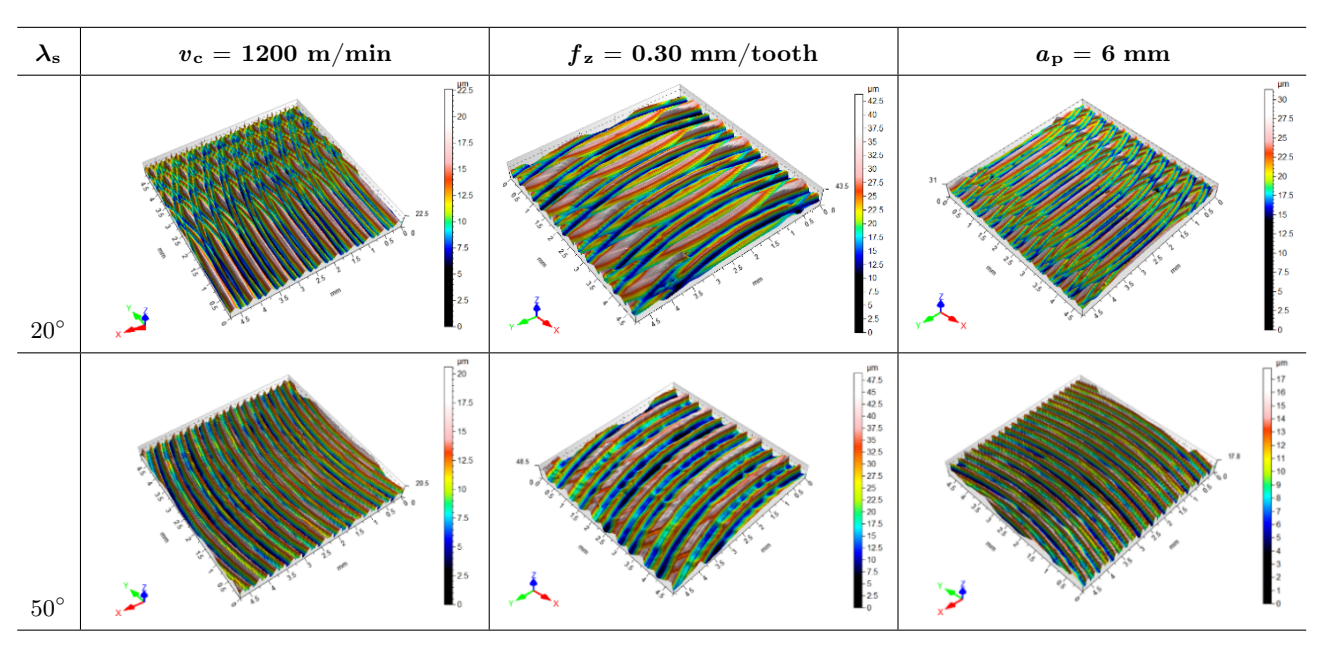


Table 6
Abbott–Firestone curves obtained using tools with different helix angles

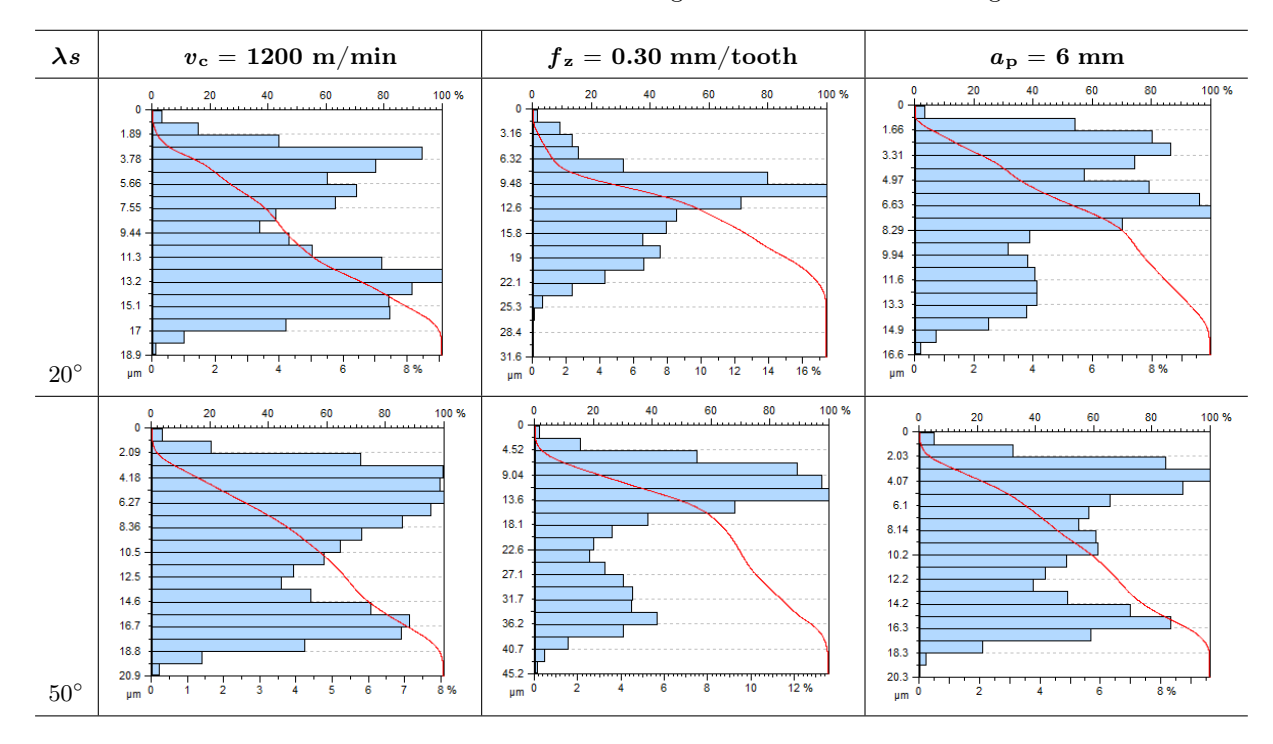


Table 7 Network parameters and results of network quality indicators for the Ra roughness parameter for end face modeling

Modeled Surface Roughness Parameter	Ra
Neurons in hidden layer	9
Epoch	123
Best validation performance	0.089 at epoch 123
Gradient	$4.19 \cdot 10^{-8}$
R (all data set)	0.966
MSE	0.096
RMSE	0.3098
MAE	0.2193

(Fig. 16), supporting these findings. The obtained values of the error indicators: MSE of 0.096, RMSE of 0.3098, and MAE of 0.2193, support the model's accuracy in predicting Ra values. These results confirm the model's reliability and suggest its strong potential for practical use in predicting surface roughness.

Numerical results of the surface roughness parameter Ra on the end face of the specimen for the variable cutting speed v_c and feed per tooth f_z are presented in

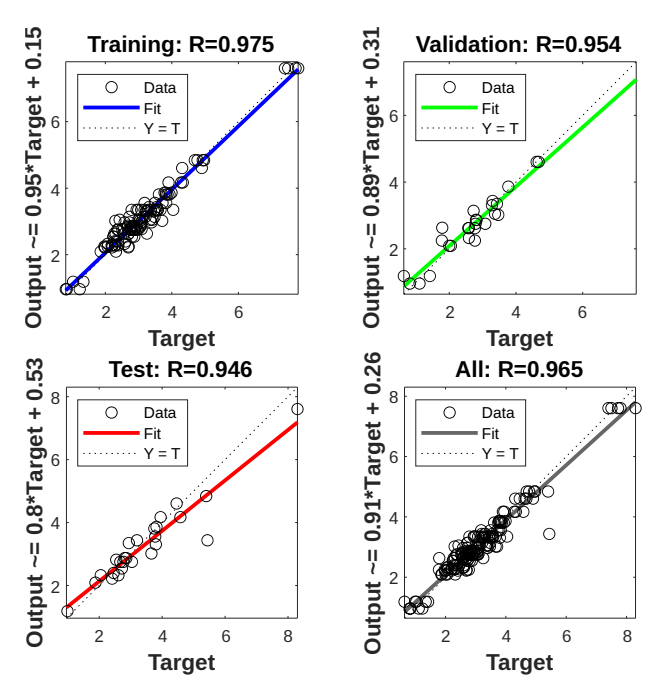


Fig. 16. Regression statistics for individual sets and the total set for the Ra roughness parameter on the end face

Figure 17a. In Figure 17b, the Ra parameter is plotted as a function of the cutting speed v_c and the axial depth of cut a_p , while in Figure 17c – it is plotted in relation to the cutting speed v_c and the helix angle λ_s .

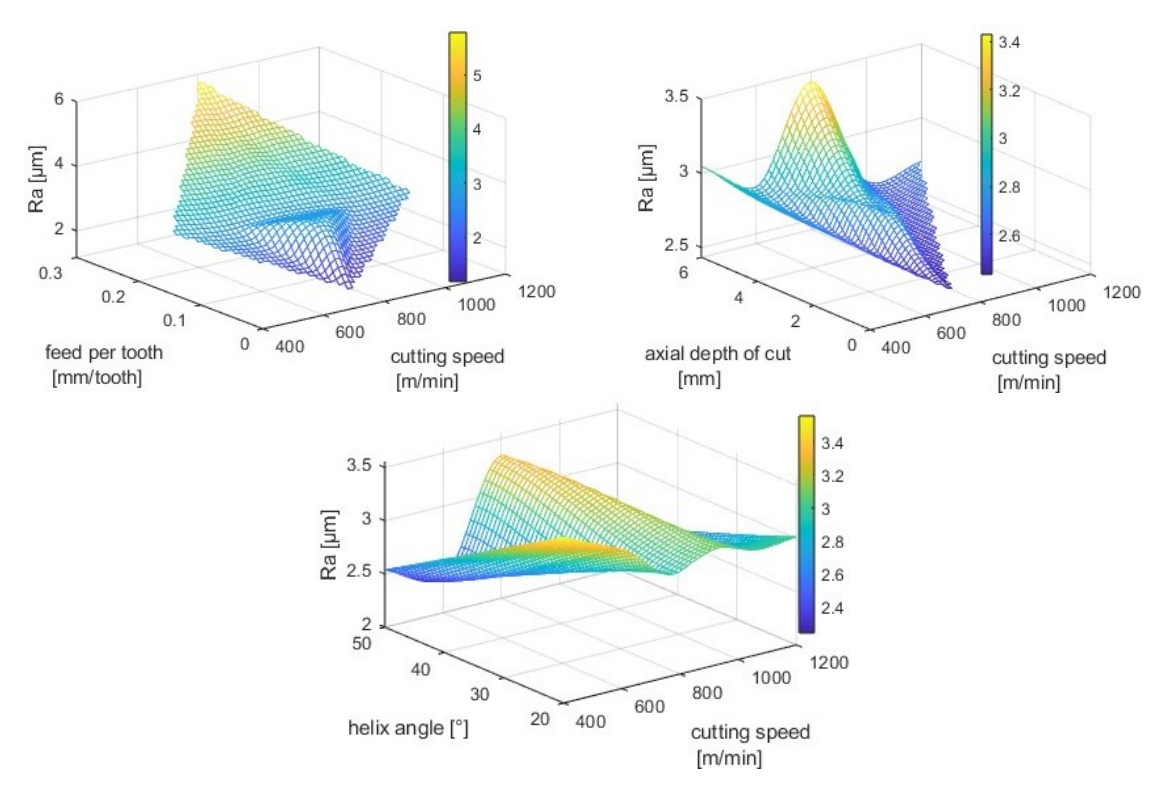


Fig. 17. Regression statistics for individual sets and the total set for the Ra roughness parameter on the end face

Discussion

The results obtained from this study on the rough milling of the AZ91D alloy are partially consistent with the findings of previous studies reported for the machining of light alloys, particularly AZ91D/HP and AZ31B. Similar trends were observed regarding the influence of technological parameters on surface roughness. As demonstrated in earlier studies, e.g. (Gziut et al., 2015), an increase in feed per tooth produced higher values of roughness parameters, while the influence of cutting speed was less direct and depended on other interacting variables, including tool geometry. This correlation was confirmed by the present study, where the use of a higher feed per tooth resulted in higher values of Ra, Rq, Rz (ANOVA results), and RSm, regardless of the tool used. It was also confirmed that the lateral surfaces would typically achieve lower roughness values than the end faces, which falls in line with earlier findings and can be attributed to the differences in effective contact zones and material removal mechanisms. A comparative analysis with the results of studies on finish milling, such as that presented in (Zagórski et al., 2022, 2024), reveals fundamental differences both in the level of roughness and in the distribution of surface features. While finish milling

typically results in significantly lower surface roughness values (often below 1 μ m for Ra and Sa), rough milling produces heterogeneous surface structures with sharper peaks and deeper valleys, which is due to its inherently more efficient material removal mechanism. This is clearly visible in the resulting 3D surface topography maps, which are characterized by distinct machining marks. Nevertheless, some parameters show similar trends, such as reduced roughness with increasing the cutting speed and higher roughness with increasing the feed per tooth. In addition, both finish and rough milling confirm that tool geometry, particularly the helix angle, plays a critical role in the surface finish treatment. In (Zagórski, 2024), the best results were obtained using tools with a rake angle of 5° and a helix angle of 50°, which is partially supported by the present results, where the 50° helix angle produced favorable results for the selected parameter ranges, particularly on the lateral face and at low f_z values (e.g., at low feed values, the tool with a larger helix angle yielded better Ra results,).

According to generally available knowledge, the use of carbide tools has its advantages over, for example, HSS tools and PCD insert tools. Compared to HSS tools, carbide tools have a significantly higher quality of workmanship (and, therefore, a sharper geometry and smaller cutting edge radius). In comparison to

PCD insert tools (whether brazed or replaceable), carbide tools are many times cheaper. To give an example, the surface roughness parameters after machining with an HSS tool can have the following values: Ra from approx. 1.5 µm to 16.125 µm (with the average value of approx. $7 \mu m$), Rz from approx. $8 \mu m$ to even approx. 80 µm (Kulisz et al., 2022a), while Sa can range from approx. 1.5 µm and does not exceed 8 µm for most cases, while Sz can range from approx. 25 µm and does not exceed 150 µm (Kulisz et al., 2022b). While the use of a PCD tool often allows for quality comparable to or even better than that achieved after finish grinding, the Ra parameter can be as low as $0.12 \mu m$ (with its average values ranging $0.2-0.4 \mu m$), while the Sa parameter is usually from 0.2 to 0.8 μ m (Zagórski & Korpysa, 2020). An important contribution of this study is the integration of the helix angle as an input variable in the artificial neural network model developed for Ra prediction. This approach represents a novel approach to the state of the art in this field, as most previous models, such as those reported in (Chen et al., 2017), excluded geometric tool parameters from the modeling process. The ANN model developed in this work demonstrated a high predictive ability, which was confirmed by the regression coefficient R = 0.966 and a low value of the mean absolute error (MAE = $0.2193 \mu m$). This proves the suitability of data-driven models for surface roughness prediction and highlights the practical potential of ANN implementation in manufacturing environments. Unlike conventional modeling approaches, ANN allows for fast and accurate prediction of machining results based on experimentally validated input combinations, thus providing a decision support tool for process engineers and technologists.

From a theoretical point of view, this study provides deep insight into the interaction between technological parameters and cutting tool geometry. The statistical analysis via ANOVA and post-hoc Tukey tests revealed that both cutting speed and feed per tooth have a significant effect on the Rz parameter. In particular, for $\lambda_s=20^\circ$, significant variations were observed in response to the variations in both v_c and f_z , whereas for $\lambda_s=50^\circ$, the dominant influence was associated with varying feed per tooth. These results contribute to the body of knowledge by demonstrating that geometric features not only influence the distribution of roughness values, but also determine the statistical sensitivity of surface to machining parameters.

The practical implications of the results from this study are equally important. They suggest that with a careful selection of tool geometry and cutting parameters, it is possible to achieve surface roughness values that eliminate the need for finish grinding in certain industrial applications. This is particularly relevant in industries such as aerospace and automotive, where magnesium alloys are increasingly used due to their low density and favorable mechanical properties. The results also show that dry machining with optimized tools can deliver surface quality within acceptable tolerances and thus support the implementation of more sustainable manufacturing practices by reducing the need for lubrication and by minimizing environmental impact.

Despite the promising results, the study has certain limitations. The research was conducted using only two discrete helix angles, and further research is needed to investigate a wider range of tool geometries, including variable helix and rake angle combinations. In addition, although both lateral and end faces were examined for the 2D parameters, the 3D surface analysis was limited to the end faces of the samples due to sample constraints. Also, the present study did not include "functional" parameters such as Rpk, Rk and Rvk, which could be useful for assessing wear resistance and adhesion behavior. Therefore, future studies should expand the scope of analysis by including additional surface functional parameters and applying the proposed methodology to ultra-light alloys, including magnesium-lithium and aluminum-lithium alloys. In addition, precision and finish milling processes merit further investigation with the use of the modeling and evaluation developed in this study.

Conclusions

The results of this research lead to the following conclusions:

- The lateral surfaces of rough-milled AZ91D magnesium alloy samples show significantly higher quality, as confirmed by several times lower values of the surface roughness parameters; for many cases, the Ra and Rq values on the lateral faces of the samples were up to 3–5 times lower than those on the end faces, which can be attributed to more favorable material flow and tool engagement conditions during lateral machining.
- The surface roughness of the samples primarily depends on the feed per tooth, an increase in its value leads to higher values of the tested roughness parameters, while the impact of the cutting speed and axial depth of cut is considerably less significant; this is particularly evident for Ra, Rz and RSm, the values of which showed a monotonic increase with increasing f_z from 0.05 to 0.30 mm/tooth.
- The obtained surface topography maps confirm

- that the use of the tool with a smaller helix angle produces surfaces with a more uniform texture; the machining marks were more regular, with fewer distortions, which probably indicated better chip evacuation and higher thermal stability in machining with $\lambda_s=20^\circ$ under higher loads.
- It is difficult to clearly indicate which helix angle value produced better surface quality because the machining effect varied greatly depending on the technological parameters; for example, at low feed values, the tool with a larger helix angle yielded better Ra results, while at higher feeds this trend was reversed, which indicates complex interactions between tool geometry and process kinematics.
- The kurtosis parameter (Sku) took values below 3 and they were only positive (which may prove that the peaks and grooves are rounded); the value exceeding 3 was only observed when the machining process was conducted using f_z of 0.05 mm/tooth and λ_s of 50°, which suggests localized peak concentration for low material removal rates with a higher helix angle.
- It is difficult to establish a clear trend for skewness (Ssk), as this parameter took both positive and negative values; the use of higher values of the machining parameters often resulted in the negative values of Ssk, the exception being the case when the machining process was conducted with v_c of 1200 m/min and λ_s of 20°, which indicates a shift from the peak-dominated to the valley-dominated profiles under more severe cutting conditions.
- The machining marks visible on the 3D surface roughness maps are typical of rough milling, and they reflect a standard heterogeneous structure with sharp peaks or deep valleys.
- The shape of the obtained Abbott–Firestone curves for the tested cutting speed was proportional. For the tested feed per tooth, it was approximately degressive-progressive (for a helix angle of 20°) or progressive (for a helix angle of 50°), and for the axial depth of cut it was progressive (for a helix angle of 20°) and approximately proportional (for a helix angle of 50°). This behavior pattern of the curves reflects the redistribution of material on the surface and the changes in peak/valley geometry due to plastic flow and chip dynamics.
- The ANOVA analysis showed statistically significant differences for the roughness parameter Rz. These differences were observed for the 20° helix angle combined with the variable cutting speed and feed per tooth and for the 50° helix angle and the variable feed per tooth, which confirms that the feed was the most dominant factor across both geometries, while the cutting speed had a signifi-

- cant impact only with lower helix angles, which is possibly due to a different chip removal dynamics.
- The results of the ANOVA analysis of variance demonstrated statistically significant differences between the mean values of the roughness parameter Rz for the analyzed groups, the post-hoc test (Tukey test, marked in red) showed the level of probability for which there were no statistically significant differences.
- The created network had a good predictive capability, as indicated by the obtained R-correlation value (R = 0.966); this shows that artificial neural networks have the potential to become an effective tool for predicting surface roughness parameters. The obtained error values, such as MSE = 0.096 and MAE = 0.2193 μm, confirm the model's reliability in practical applications.
- The trained networks serve as a helpful tool for technologists in establishing machining parameters to attain the precise surface roughness; they can reduce the number of trial experiments, shorten machining time and help ensure reproducibility of the desired surface quality even in dry conditions.

Acknowledgments

The project/research was financed with FD-20/IM-5/138, FD-20/IM-5/061, FD-20/IM-5/144 and FD-20/IM-5/107.

References

Adhikari, R., Bolar, G., Shanmugam, R., & Koklu, U. (2023). Machinability and surface integrity investigation during helical hole milling in AZ31 magnesium alloy. *International Journal of Lightweight Materials and Manufacture*, 6(2), 149–164. DOI: 10.1016/J.IJLMM.2022.09.006

Ahmed, F., Ahmad, F., Abbassi, F., Kumaran, S.T., & Mabrouki, T. (2023). Investigation of machining quality indicators and effect of tool geometry parameters during the machining of difficult-to-machine metal. *Results in Materials*, 20, 100487. DOI: 10.1016/J.RINMA.2023.100487

Bari, P., Kilic, Z.M., & Law, M. (2023). Rapid stability analysis of variable pitch and helix end mills using a non-iterative multi-frequency solution. *Proceedings of the Institution of Mechanical Engineers, Part B: Journal of Engineering Manufacture, 237*(13), 2109–2118.

- Biruk-Urban, K., Józwik, J., & Bere, P. (2022). Cutting Forces and 3D Surface Analysis of CFRP Milling. Advances in Science and Technology. Research Journal, 16(2), 206–215. DOI: 10.12913/22998624/147338
- Chen, Y., Sun, R., Gao, Y., & Leopold, J. (2017). A nested-ANN prediction model for surface roughness considering the effects of cutting forces and tool vibrations. *Measurement*, 98, 25–34. DOI: 10.1016/J.MEASUREMENT.2016.11.027
- Dijmărescu, M.R., Abaza, B.F., Voiculescu, I., Dijmărescu, M.C., & Ciocan, I. (2021). Surface Roughness Analysis and Prediction with an Artificial Neural Network Model for Dry Milling of Co–Cr Biomedical Alloys. *Materials*, 14(21), 6361. DOI: 10.3390/MA14216361
- El-Shenawy, E.H., & Farahat, A.I.Z. (2023). Surface quality and dry sliding wear behavior of AZ61Mg alloy using Abbott firestone technique. *Scientific Reports* 2023, 13(1), 1–18. DOI: 10.1038/s41598-023-39413-x
- Ercetin, A., Aslantaş, K., Özgün, Ö., Perçin, M., &Chandrashekarappa, M.P.G. (2023). Optimization of Machining Parameters to Minimize Cutting Forces and Surface Roughness in Micro-Milling of Mg13Sn Alloy. *Micromachines*, 14(8), 1590. DOI: 10.3390/MI14081590
- Gziut, O., Kuczmaszewski, J., & Zagórski, I. (2015). Surface quality assessment following high performance cutting of AZ91HP magnesium alloy. Management and Production Engineering Review, 6(1), 4–9. DOI: 10.1515/MPER-2015-0001
- Hu, X., Qiao, H., Yang, M., & Zhang, Y. (2022). Research on Milling Characteristics of Titanium Alloy TC4 with Variable Helical End Milling Cutter. *Machines*, 10(7), 537. DOI: 10.3390/MACHINES10070537
- Jouini, N.;, Ruslan, M.;, Ghani, J. A.;, Haron, C., Murad, M.N., Jouini, N., Shahfizal, M., Ruslan, M., Ghani, J.A., & Hassan, C. (2023). Sustainable High-Speed Milling of Magnesium Alloy AZ91D in Dry and Cryogenic Conditions. Sustainability, 15(4), 3760. DOI: 10.3390/SU15043760
- Kanan, M., Zahoor, S., Habib, M.S., Ehsan, S., Rehman, M., Shahzaib, M., Khan, S.A., Ali, H., Abusaq, Z., & Hamdan, A. (2023). Analysis of Carbon Footprints and Surface Quality in Green Cutting Environments for the Milling of AZ31 Magnesium Alloy. Sustainability, 15(7), 6301. DOI: 10.3390/SU15076301
- Karmiris-Obratański, P., Karkalos, N.E., Kudelski, R., & Markopoulos, A. P. (2022). Experimental study on the effect of the cooling method on surface topography and workpiece integrity during trochoidal end milling of Incoloy 800. Tribology International, 176, 107899. DOI: 10.1016/J.TRIBOINT.2022.107899

- Kaviarasan, V., Venkatesan, R., & Natarajan, E. (2019).
 Prediction of surface quality and optimization of process parameters in drilling of Delrin using neural network. Progress in Rubber, Plastics and Recycling Technology, 35(3), 149-169. DOI: 10.1177/1477760619855078
- Khawaja, A.H., Jahanzaib, M., &Cheema, T.A. (2020). High-speed machining parametric optimization of 15CDV6 HSLA steel under minimum quantity and flood lubrication. Advances in Production Engineering And Management, 15(4), 403–415. DOI: 10.14743/APEM2020.4.374
- Kramar, D., & Cica, D.J. (2021). Modeling and optimization of finish diamond turning of spherical surfaces based on response surface methodology and cuckoo search algorithm. Advances in Production Engineering And Management, 16(3), 326-334. DOI: 10.14743/APEM2021.3.403
- Krzyzak, A., Kosicka, E., Borowiec, M., & Szczepaniak, R. (2020). Selected Tribological Properties and Vibrations in the Base Resonance Zone of the Polymer Composite Used in the Aviation Industry. *Materials*, 13(6), 1364. DOI: 10.3390/MA13061364
- Kuczmaszewski, J., Pieśko, P., & Zawada-Michałowska, M. (2016). Surface roughness of thin-walled components made of aluminium alloy EN AW-2024 following different milling strategies. Advances in Science and Technology. Research Journal, 10(30), 150-158. DOI: 10.12913/22998624/62515
- Kulisz, M., Zagórski, I., & Józwik, J. (2022a). 2D Geometric Surface Structure ANN Modeling after Milling of the AZ91D Magnesium Alloy. Advances in Science and Technology. Research Journal, 16(2), 131–140. DOI: 10.12913/22998624/146765
- Kulisz, M., Zagórski, I., Józwik, J., & Korpysa, J. (2022b). Research, Modelling and Prediction of the Influence of Technological Parameters on the Selected 3D Roughness Parameters, as Well as Temperature, Shape and Geometry of Chips in Milling AZ91D Alloy. Materials, 15(12), 4277. DOI: 10.3390/MA15124277
- Kumar, R., Katyal, P., & Kumar, K. (2023). Effect of End Milling Process Parameters and Corrosion Behaviour of ZE41A Magnesium Alloy using Taguchi Based GRA. Biointerface Research in Applied Chemistry, 13(3), 214. DOI: 10.33263/BRIAC133.214
- Lisowicz, J., Habrat, W., & Krupa, K. (2022). Influence of Minimum Quantity Lubrication Using Vegetable-Based Cutting Fluids on Surface Topography and Cutting Forces in Finish Turning of Ti-6Al-4V. Advances in Science and Technology. Research Journal, 16(1), 95–103. DOI: 10.12913/22998624/143289

- Marakini, V., Pai, S.P., Bhat, U.K., Thakur, D.S., & Achar, B.P. (2022). High-speed face milling of AZ91 Mg alloy: Surface integrity investigations. International Journal of Lightweight Materials and Manufacture, 5(4), 528–542. DOI: 10.1016/J.IJLMM. 2022.06.006
- Matuszak, J. (2023). Analysis of Geometric Surface Structure and Surface Layer Microhardness of Ti6Al4V Titanium Alloy after Vibratory Shot Peening. Materials, 16 (21), 6983. DOI: 10.3390/MA16216983
- Matuszak, J., Kłonica, M., Zagórski, I. (2019). Effect of brushing conditions on axial forces in ceramic brush surface treatment. 2019 IEEE International Workshop on Metrology for AeroSpace, MetroAeroSpace 2019 – Proceedings, 2019, 644–648, 8869605
- Niemczewska-Wójcik, M., & Madej, M. (2023). Surface Topography and Tribological Properties of Cutting Tool Coatings. Advances in Science and Technology. Research Journal, 17(6), 39–48. DOI: 10.12913/22998624/173214
- Sangwan, K.S., Saxena, S., & Kant, G. (2015). Optimization of Machining Parameters to Minimize Surface Roughness using Integrated ANN-GA Approach. Procedia CIRP, 29, 305–310. DOI: 10.1016/J.PROCIR. 2015.02.002
- Savkovic, B., Kovac, P., Rodic, D., Strbac, B., & Klancnik, S. (2020). Comparison of artificial neural network, fuzzy logic and genetic algorithm for cutting temperature and surface roughness prediction during the face milling process. Advances in Production Engineering And Management, 15(2), 137–150. DOI: 10.14743/APEM2020.2.354
- Sur, G., Motorcu, A.R., &Nohutçu, S. (2022). Single and multi-objective optimization for cutting force and surface roughness in peripheral milling of Ti6Al4V using fixed and variable helix angle tools. *Journal* of Manufacturing Processes, 80, 529–545. DOI: 10.1016/J.JMAPRO.2022.06.016
- Tomov, M., Gecevska, V., &Vasileska, E. (2022). Modelling of multiple surface roughness parameters during hard turning: A comparative study between the kinematical-geometrical copying approach and the design of experiments method (DOE). Advances in Production Engineering And Management, 17(1), 75–88. DOI: 10.14743/APEM2022.1.422
- Varatharajulu, M., Duraiselvam, M., Krishna Pradeep, G.V., & Jagadeesh, B. (2023). Tool temperature thermographic study on end milling magnesium AZ31 using carbide tool. *Materials Chemistry* and Physics, 295, 127077. DOI: 10.1016/J.MATCHEM PHYS.2022.127077

- Vukelic, D., Simunovic, K., Kanovic, Z., Saric, T., Doroslovacki, K., Prica, M., & Simunovic, G. (2022). Modelling surface roughness in finish turning as a function of cutting tool geometry using the response surface method, Gaussian process regression and decision tree regression. Advances in Production Engineering And Management, 17(3), 367–380. DOI: 10.14743/APEM2022.3.442
- Wang, C., Chen, C., Huang, Z., Zhao, J., & Yang, E. (2023). Influence of milling parameters on machining performances and surface quality of ZK61M magnesium alloy. *International Journal of Advanced Manufacturing Technology*, 128(11–12), 4777–4789. DOI: 10.1007/S00170-023-12241-Z/FIGURES/14
- Xue, K., Chen, P., Liu, W., Zou, B., Li, L., Chen, W., Wang, X., & Xu, Z. (2023). Geometric Structures for Sialon Ceramic Solid End Mills and Its Performance in High-Speed Milling of Nickel-Based Superalloys. Coatings, 13(9), 1483. DOI: 10.3390/COATINGS13091483
- Zagórski, I. (2024a). Surface Roughness of Magnesium Alloy AZ91D after Rough Milling Using Carbide End Mills with Different Rake Angle. 2024 IEEE International Workshop on Metrology for AeroSpace, MetroAeroSpace 2024 - Proceeding, 57–62. DOI: 10.1109/METROAEROSPACE61015.2024.10591602
- Zagórski, I. (2023). Safety in Rough Milling of Magnesium Alloys Using Tools with Variable Cutting Edge Geometry. Advances in Science and Technology. Research Journal, 17(2), 181–191. DOI: 10.12913/ 22998624/159637
- Zagórski, I. (2024b). Surface Roughness Evaluation of AZ31B Magnesium Alloy After Rough Milling Using Tools with Different Geometries. Strojniški Vestnik – Journal of Mechanical Engineering, 70 (7–8), 355–368. DOI: 10.5545/SV-JME.2023.885
- Zagórski, I., & Korpysa, J. (2020). Surface Quality Assessment after Milling AZ91D Magnesium Alloy Using PCD Tool. *Materials*, 13(3), 617. DOI: 10.3390/ma13030617
- Zagórski, I., Kulisz, M., & Szczepaniak, A. (2024). Roughness Parameters with Statistical Analysis and Modelling Using Artificial Neural Networks After Finish Milling of Magnesium Alloys with Different Edge Helix Angle Tools. StrojniskiVestnik/Journal of Mechanical Engineering, 70(1–2), 27–41. DOI: 10.5545/SV-JME.2023.596
- Zagórski, I., Szczepaniak, A., Kulisz, M., & Korpysa, J. (2022). Influence of the Tool Cutting Edge Helix Angle on the Surface Roughness after Finish Milling of Magnesium Alloys. *Materials*, 15(9), 3184. DOI: 10.3390/MA15093184

- Zawada-Michałowska, M., Kuczmaszewski, J., & Pieśko, P. (2020). Pre-Machining of Rolled Plates as an Element of Minimising the Post-Machining Deformations. Materials, 13 (21), 4777. DOI: 10.3390/MA13214777
- Zawada-Michałowska, M., Kuczmaszewski, J., & Pieśko, P. (2022). Effect of the Geometry of Thin-Walled Aluminium Alloy Elements on Their Deformations after Milling. *Materials*, 15 (24), 9049. DOI: 10.3390/MA15249049
- Zawada-Michałowska, M., Pieśko, P., & Legutko, S. (2023). Effect of the Cutting Tool on the Quality of a Machined Composite Part. Manufacturing Technology, 23(6), 870–879. DOI: 10.21062/MFT.2023.107
- Zhang, P., Huang, Y., Wang, R., & Ohashi, K. (2023). Study of Machined Surface Quality of AZ31B Magnesium Alloy by End Milling. *Metals*, 13(10), 1712. DOI: 10.3390/MET13101712